Controlled release of methyl salicylate by biosorbents delays the ripening of banana fruit

Chalida Cholmaitri [1] , **Apiradee Uthairatanakij** [Corresp., 1] , **Natta Laohakunjit** [2] , **Pongphen Jitareerat** [1] , **Withawat Mingvanish** [3]

[1] Postharvest Technology, King Mongkut's University of Technology Thonburi, Bangkok, Thailand

[2] Biochemical Technology, King Mongkut's University of Technology Thonburi, Bangkok, Thailand

[3] Department of Chemistry, King Mongkut's University of Technology Thonburi, Bangkok, Thailand

Corresponding Author: Apiradee Uthairatanakij
Email address: apiradee.uth@kmutt.ac.th

The efficiencies of rice flour (RF) and rice husk (RH) as agents of the controlled release of methyl salicylate (RF-MeSA and RH-MeSA, respectively) were investigated. The adsorption percentage of RH-MeSA was significantly higher (2-fold) than that of RF-MeSA owing to its higher specific surface area and total pore volume. However, both materials are classified as mesoporous materials. Scanning electron microscopy (SEM), X-ray diffraction (XRD), Fourier transform infrared (FTIR) spectroscopy, and thermogravimetric analysis (TGA) confirmed that MeSA diffused toward the pores and covered the surfaces of RF and RH. A temperature increase from 25 °C to 40 °C and an increase in relative humidity from 75 % to 95 % stimulated the release of MeSA. The kinetically controlled release of RF-MeSA and RH-MeSA was in line with a Fickian diffusion mechanism. Both RF-MeSA and RH-MeSA significantly delayed the ripening of banana fruit compared to the control. The results indicate that RF and RH can be used as biosorbent materials for the adsorption and controlled release of MeSA without chemical and mechanical modification.

1   # Manuscript Title

2   **Controlled release of methyl salicylate by biosorbents delays the ripening of banana fruit**

3   Chalida Cholmaitri[1], Apiradee Uthairatanakij[1,] Natta Laohakunjit[2], Pongphen Jitareerat[1],

4   Withawat Mingvanish[3]

5   [1]Division of Postharvest Technology, School of Bioresources and Technology, King Mongkut's

6   University of Technology Thonburi (Bangkhuntien), Bangkok 10150, Thailand

7   [2]Division of Biochemical Technology, School of Bioresources and Technology, King Mongkut's

8   University of Technology Thonburi (Bangkhuntien), Bangkok 10150, Thailand

9   [3]Department of Chemistry, King Mongkut's University of Technology Thonburi, Bangkok

10   10140, Thailand

12   Corresponding Author:

13   Apiradee Uthairatanakij[1]

14   [1]Division of Postharvest Technology, School of Bioresources and Technology, King Mongkut's

15   University of Technology Thonburi (Bangkhuntien), Bangkok 10150, Thailand

16   Email address: apiradee.uth@kmutt.ac.th

Abstract

The efficiencies of rice flour (RF) and rice husk (RH) as agents of the controlled release of

methyl salicylate (RF-MeSA and RH-MeSA, respectively) were investigated. The adsorption

percentage of RH-MeSA was significantly higher (2-fold) than that of RF-MeSA owing to its

higher specific surface area and total pore volume. However, both materials are classified as

mesoporous materials. Scanning electron microscopy (SEM), X-ray diffraction (XRD), Fourier

transform infrared (FTIR) spectroscopy, and thermogravimetric analysis (TGA) confirmed that

MeSA diffused toward the pores and covered the surfaces of RF and RH. A temperature increase

from 25 °C to 40 °C and an increase in relative humidity from 75 % to 95 % stimulated the

release of MeSA. The kinetically controlled release of RF-MeSA and RH-MeSA was in line with

a Fickian diffusion mechanism. Both RF-MeSA and RH-MeSA significantly delayed the

ripening of banana fruit compared to the control. The results indicate that RF and RH can be

used as biosorbent materials for the adsorption and controlled release of MeSA without chemical

and mechanical modification.

Introduction

Physiological and biochemical changes during fruit ripening lead to changes in color, a peak in

respiration, a burst in ethylene production, softening and declines in acidity (Gray et al, 1994).

Ethylene is an endogenous plant hormone responsible for fruit ripening and senescence (Pratt &

Goeschl, 1969). Ethylene is synthesized from methionine through the intermediaries S-adenosyl

methionine (SAM) and 1-aminocyclopropane-1-carboxylic acid (ACC). The enzyme that

converts methionine to SAM is SAM synthase, while ACC synthase converts SAM to ACC, and

ACC oxidase catalyzes the oxidation of ACC to ethylene (Yang & Hoffman, 1984).

46   Methyl salicylate (MeSA) is a volatile organic compound that plays an important role in

47   inhibiting the activity of ACC synthase and ACC oxidase in tomatoes and plums (Ding et al.,

48   2002; Khan, Singh & Abbasi, 2007). It delays the postharvest ripening process in papayas,

49   mangos, and sweet peppers (González-Aguilar, Buta & Wang, 2003; Fung et al., 2004; Han et

50   al., 2006). Moreover, it has a strong ability to inhibit fungal infections and reduce chilling injury

51   symptoms (Ryals et al., 1996; Fung et al., 2006; Min et al., 2018). MeSA is used as a food

52   additive that is classified by the U.S. Food and Drug Administration as a Generally Recognized

53   as Safe (GRAS) substance (Chanjirakul et al., 2006). Fumigation with 1.0 mmolL^{-1} of MeSA

54   vapor for 16 h at 20 °C reduced the weight loss, respiration rate, softening and total acidity of

55   sweet cherries (Giménez et al., 2016). MeSA vapor at 0.5 mmolL^{-1} for 16 h at 23 °C prevented

56   red color development, ethylene production and respiration in tomatoes (Ding & Wang, 2003).

57   Moreover, pomegranates dipped in 1.0 mmolL^{-1} MeSA showed a significant reduction in chilling

58   injury and maintained quality and health when stored at 2 °C for 3 months (Sayyari et al., 2011).

59   Chotikakham et al. (2019) found that bananas dipped in MeSA solution at concentrations of 2

60   and 4 mmolL^{-1} maintained fruit quality and reduced peel spotting.

61   MeSA is usually applied to fruit either by fumigation or by dipping them in a solution

62   (Srivastava & Dwivedi, 2000; Bagnato et al., 2003). However, these applications are limited in

63   their efficacy because of the rapid release of this volatile organic compound (Mir et al., 2014). A

64   controlled release system that can slow the release of active compounds has been applied to

65   prolong shelf life and control the quality of meat, fish, poultry, bread, cheese, beverages, fruit,

66   and vegetables (López-Rubio et al., 2004). Factors affecting controlled release include the

67   coating materials (pore size, wall thickness, and coating layers), type of active compound or

68   core, and the release environment (temperature, and relative humidity) (Yebra, Kiil & Dam-

69   Johansen, 2004; Hoffman, 2008; Vilar, Tulla-Puche & Albeicio, 2012).

70   A number of biosorbent materials, such as α-cyclodextrin (α-CD), β-cyclodextrin (β-CD),

71   activated carbon, and zeolite are used in controlled release techniques (Kamada et al., 2002;

72   Hamadi, Swaminathan & Chen, 2004; Fernández-Pérez et al., 2005; Namazi, Bahrami &

73   Entezami, 2005; Trichard et al., 2007; Fatouros et al., 2011). A 1-methylcyclopropene (1-

74   MCP)/α-CD inclusion complex powder has been shown to delay the ripening and prolong the

75   shelf life of tomato (Ariyanto, Bercis & Yoshii, 2019). β-CD inclusion with hexanal has been

76   shown to inhibit postharvest disease in berries (Almenar et al., 2007). In addition, activated

77   carbon with ethanol has been shown to prevent microbial contamination of strawberries

78   (Kawagoe, Takikawa & Hikosaka 1998). Zeolite is used as a fertilizer carrier to control the

79   release of nitrate (Li, 2003), phosphate (Bansiwal et al., 2006), and sulfate (Li & Zhang, 2010).

80   Cyclodextrins (CDs), which are produced during the degradation of starch by enzymatic

81   conversion, are water-soluble, with a hydrophobic interior and hydrophilic exterior (Cevallos,

82   Buera & Elizalde, 2010). They are used to coat or encapsulate insoluble compounds (Teranishi &

83   Shimomura, 2014). However, biosorbent materials that are used to slow the ripening process and

84   reduce postharvest loss need to be water-insoluble. For example, cellulose is a natural

85   biopolymer that is water-insoluble, but with a highly charged and, thus, modifiable surface

86   (Bochek, 2003). Therefore, the use of agricultural by-products and wastes as biosorbent

87   materials is becoming an area of interest because they are renewable and low-cost. The

88   characteristics of various types of starches, such as a double-helix of linear amylose molecules

89   have the ability to bind with other hydrophobic molecules such as iodine, fatty acids, or aromatic

90   compounds, make them potential candidates for applications related to adsorption and controlled

91   release (Geera et al., 2006). Potato and corn starch can adsorb volatile compounds (Bermiller &

92   Pratt, 1981), and amylose extracted from potato starch can bind with *n*-butyl alcohol, iso-amyl

93   alcohol, menthone, and other compounds (Takeo & Kuge, 1969). Moreover, rice starch has been

94   used as an ingredient in dry shampoo because it absorbs oil in the hair (Santander-Ortega et al.,

95   2010). Assam Bora rice starch can be used as a carrier for controlled-release drug delivery

96   (Ahmad et al., 2012). Rice starch-konjac glucomannan (KGM) blend films with MeSA have

97   shown potential as agents of controlled release of bioactive compounds (Satirapipathkul &

98   Meesukanun, 2013).

99   Rice husk (RH), an agricultural waste product that is generated in the milling process of rice

100   grain, is normally used as feed for livestock. The major constituents of RH are cellulose (35 %),

101   lignin (25 %), silica (20 %), crude protein (3 %), and ash (17 %) (Ugheoke & Mamat, 2012). The

102   latter constituent imbues the husks with high surface area and porosity, two important attributes

103   that facilitate adsorption and desorption (Basha et al., 2005). Rice husk ash (RHA) is a source of

104   silica, which is used in slow-release drug delivery systems (Prawingwong et al., 2009). Urea

105   coated with rice husk charcoal (RHC) has the potential to slow the release of nitrogen fertilizer

106   (Xiaoyu et al., 2013). To the best of our knowledge, there are no reports in the literature that

107   examine the applicability of RF and RH to the adsorption and controlled release of MeSA.

108   Therefore, the objectives of this study were to investigate the efficacy of RF and RH without a

109   modified surface in adsorbing MeSA and their ability to slowly release this compound, as well as

110   to understand the release kinetics of these two biosorbents. RF and RH biosorbents were used to

111   examine the delay in fruit ripening, using bananas as a model. Bananas are a climacteric fruit

112   which show a sharp increase in ethylene production with a high respiration rate during the time

113 of ripening (Bouzayen et al., 2010). These two biosorbents can potentially be applied in

114 postharvest technology as an environmentally friendly method of delaying fruit ripening.

115

116 **Materials and Methods**

117 **Preparation and characterization of biosorbents**

118 **Materials**

119 Rice flour, derived from broken rice (*Oryza sativa* L.), was purchased from a local market in

120 Ratchaburi Province, Thailand. The amylose content was 30.2 % and the moisture content was

121 10.1 %. Rice husk was supplied by Nugreen Co., Ltd. (Thailand), and had a moisture content of

122 7.6 %. Moisture contents were determined following the method of the Association of Official

123 Analytical Chemists (AOAC, 2000). The RF and RH were ground into powder using a grinder

124 (Cuisinart SG-10 HK, China), then dried at 60 °C for 96 h in a hot air oven to remove moisture.

125 The powders were passed through 0.250-0.177 mm sieve and kept in a desiccator until they were

126 used for physical characterization and study of adsorption and desorption properties. Methyl

127 salicylate (MeSA; purity $\geq$ 99 %) was obtained from Sigma-Aldrich (St. Louis, MO, USA).

128

129 **Measurement of Brunauer-Emmett-Teller (BET) surface areas**

130 The specific surface area, total pore volume, and average pore diameter of RF and RH powder

131 (0.250-0.177 mm) were determined by nitrogen sorption at 77 K using a Brunauer-Emmett-

132 Teller (BET) surface analyzer (Model Quantachrome, Autosorb 1, Boynton Beach, Florida,

133 USA). The surface area was determined according to the BET equation (Brunauer, Emmett &

134 Teller 1983).

135

136 **Adsorption of rice flour-methyl salicylate (RF-MeSA) and rice husk-methyl salicylate (RH-**

137 **MeSA)**

138 The biosorbents (RF and RH) were weighed and placed into 10 mL airtight glass vials. MeSA

139 was added to each of the biosorbents at a ratio of 2:1 (w/w; MeSA: biosorbent) and left at 25 °C

140 for 24 h. The adsorption percentage and physical characteristics of RF-MeSA and RH-MeSA

141 were then assessed.

142

143 **Adsorption percentage**

144 The RF-MeSA and RH-MeSA mixtures were filtered using Whatman® filter paper No. 1 to remove

145 excess MeSA (Mulugeta & Lelisa, 2014) and weighed at 0, 1, 2, 3, 6, 12, and 24 h to determine

146 the adsorption percentage of RF-MeSA and RH-MeSA. The adsorption percentage was calculated

147 as follows:

148 $$\text{Adsorption (\%)} = [(W_i - W_t)/W_i] \times 100 \qquad\qquad (1)$$

149 where W_i is the adsorbed weight at the initial time (g) and W_t is the adsorbed weight at time t (g).

150

151 **Scanning electron microscopy (SEM) and energy dispersive X-ray spectroscopy (EDS)**

152 Samples of RF, RH, RF-MeSA, and RH-MeSA were mounted on stubs using adhesive carbon

153 tape and coated with gold. The morphology was investigated using a scanning electron

154 microscope (SEM-EDS; JSM 6610 LV, JEOL Ltd., Tokyo, Japan) at 2,500× magnification and

155 an accelerating voltage of 10 kV.

156

157 **X-ray diffraction (XRD)**

158   The X-ray patterns of RF, RH, RF-MeSA, and RH-MeSA samples (0.5 g) were analyzed using

159   an XRD analyzer (Bruker AXS, Model D8 Discover, Billerica, MA, USA) with copper radiation

160   at a voltage of 40 kV and 40 mA. The RF, RH, RF-MeSA, and RH-MeSA samples were scanned

161   between $2\theta = 5°-60°$ with a scanning speed of $2°$ min^{-1}.

162

163   **Fourier transform infrared (FTIR) spectroscopy**

164   For functional group analysis, 2 mg samples of RF, RH, RF-MeSA, and RH-MeSA were mixed

165   with 100 mg of potassium bromide powder; the mixture was compressed at 10 psi. The pellets

166   were transferred into a FTIR spectrometer (Perkin Elmer, Spectrum One, USA), and their spectra

167   were recorded at a resolution of 4 cm^{-1} in a range of 400-4000 cm^{-1}.

168

169   **Thermogravimetric analysis (TGA)**

170   To determine thermal decomposition of RF, RH, RF-MeSA, and RH-MeSA, 5 mg samples were

171   scanned using a TGA analyzer (Perkin-Elmer, Model Pyris Diamond, USA). The samples were

172   heated from 30 °C to 800 °C, with a temperature ramp rate of 10 °C min^{-1}. Nitrogen was used as

173   the purge gas at a flow rate of 10 mL min^{-1}.

174

175   **Desorption of rice flour-methyl salicylate (RF-MeSA) and rice husk-methyl salicylate (RH-**

176   **MeSA)**

177   The biosorbents (RF and RH) were weighed and placed into 10 mL glass vials with aluminum

178   caps. MeSA was added to each of the biosorbents at a ratio of 2:1 (w/w; MeSA:biosorbent) and

179   left at 25 °C for 24 h. Samples of RF-MeSA and RH-MeSA (1.0 g) were placed into 10 mL

180   airtight glass vials and used to study the effect of temperature and relative humidity on

181   desorption processes.

182

183   **Effect of temperatures on desorption**

184   Samples of RF-MeSA and RH-MeSA (1.0 g) in 10 mL airtight glass vials were heated using a

185   heating box (Gemmy DB-006E, Taipei, Taiwan) at 25 °C and 40 °C respectively, at 70-75 %

186   relative humidity. Methyl salicylate gas (5 mL) from the headspace was assayed at 0, 1, 2, 3, 6,

187   9, 12, and 24 h after heating commenced by gas chromatography (GC; GC-14B Shimadzu,

188   Japan). The GC was equipped with a DB-5 column (30 m × 0.250 mm) and a flame ionization

189   detector. The column temperature was 50 °C for 5 min, then heated to 130 °C at 12 °C min^{-1}, and

190   then increased to 200 °C at 15 °C min^{-1}. Helium was used as the carrier gas at a flow rate of 1.0

191   mL min^{-1}. Injection and detector temperatures were set at 250 °C and 240 °C, respectively.

192   Methyl salicylate was used as a standard compound. The percentage desorption of MeSA was

193   calculated as follows:

194   Desorption (%) = A_t/A_{eq} × 100   (2)

195   where A_t is the peak area of MeSA at time t and A_{eq} is peak area of MeSA at equilibrium.

196

197   **Effect of relative humidity on desorption**

198   Samples of RF-MeSA and RH-MeSA (1.0 g) in 10 mL glass vials were placed in desiccators that

199   were pre-equilibrated with saturated solution sodium chloride and potassium sulfate to attain

200   relative humidities of 75 % and 95 %, respectively, at 25 °C (Greenspan, 1977). The equilibrium

201   time for the samples in the desiccator was 1 h. Headspace gas (5 mL) was collected in 1 min

202   intervals and removed at 0, 1, 2, 3, 6, 9, 12, and 24 h for the analysis of MeSA gas by GC.

203

Release kinetics

205 The release kinetics of MeSA from RF-MeSA and RH-MeSA were investigated according to the

206 methods of Ho, Joyce & Bhandari (2011) with some modifications.

207 The Korsmeyer-Peppas model (Korsmeyer et al., 1983) was employed to describe the release

208 kinetics by Eq. 3.

209 $\quad$ $M_t/M_\infty = kt^n$ $\hspace{6cm}$ (3)

210 where M_t and M_∞ represent MeSA released at time t and at equilibrium, respectively; k is the rate

211 constant; and n is the release exponent calculated from the slope of the straight line. Controlled

212 release was further evaluated by other models. First, the data were assessed as a zero-order

213 reaction (Eq. 4), as the cumulative amount of MeSA released vs. time:

214 $\quad$ $C = k_0 t$ $\hspace{6cm}$ (4)

215 where k_0 is the zero-order rate constant expressed in units of concentration/time and t is the time

216 in hours. Second, the data were assessed as a first order reaction (Eq. 5) as the log cumulative

217 percentage of MeSA remaining vs. time:

218 $\quad$ $\log C = \log C_0 - kt / 2.303$ $\hspace{5cm}$ (5)

219 where C_0 is the initial concentration of MeSA released, k is the first-order constant, and t is the

220 time in hours. Lastly, the data were assessed using the Higuchi model (Eq. 6) as the cumulative

221 percentage of MeSA released vs. square root of time:

222 $\quad$ $Q = kt^{1/2}$ $\hspace{6cm}$ (6)

223 where k is the rate constant and t is the time in hours.

224

225 **Application of rice flour-methyl salicylate (RF-MeSA) and rice husk-methyl salicylate (RH-**

226 **MeSA) on banana fruit**

227 Banana (*Musa sapientum* L. 'Namwa') fruit that were free of physical damage and symptoms of

228 disease, and were at 90 d after bloom, were collected from commercial orchards located in

229 Ratchaburi Province, Thailand. Hands were cut into individual fingers, washed with tap water,

230 dipped for 5 min in sodium-hypochlorite (200 mg L^{-1}), and air-dried at 25 ± 2 °C before

231 treatment. For each treatment, two fruit were placed inside a perforated polypropylene (PP) tray

232 (4 holes, 2.0 mm perforations), with 1.0 g of RF-MeSA or RH-MeSA in Whatman® filter paper

233 No. 1; a group without any biosorbent was used as a control. The storage period was 5 d at 25 ± 2

234 °C and at a relative humidity of 75 %. The samples were withdrawn for analysis at 0, 1, 3, and 5

235 d after initiation of the storage period. Six replicates were conducted per treatment, with two fruit

236 per package.

237 Ethylene production and respiration rate were determined by placing one banana fruit in a 600

238 mL air-tight plastic container and incubating at 25 ± 2 °C for 1 h. A 1.0 mL sample of headspace

239 gas was withdrawn and injected into the gas chromatograph (GC-2014B, Shimadzu, Japan). The

240 ethylene production is expressed as ng kg^{-1} s^{-1} and the respiration rate is expressed as µg kg^{-1} s^{-1}.

241 The color change of the banana peel was measured in three locations on each fruit using a

242 colorimeter (CR-300, Minolta, Tokyo, Japan). The measurements were expressed as yellowness

243 (*b** value). Fruit firmness was measured by a texture analyzer (TA-XT plus, Stable Micro

244 Systems, UK), and the results were expressed as force (N).

245 The half-life ($t_{1/2}$) release, which indicated the time it took for 50 % of the active compound to

246 release from the biosorbent, was determined by Eq. 7 (Ho, Joyce & Bhandari, 2011)

247 $$t_{1/2 =} \exp(-(lnk+ln(0.5))/n) \tag{7}$$

248   where k is the rate constant and n is the release exponent calculated from the slope.

249

250   **Statistical analysis**

251   All experiments were arranged in a randomized complete block design (RCBD) with three

252   replicates. The data were analyzed by analysis of variance (ANOVA) using SAS (SAS Institute;

253   Cary, NC, USA); significant differences ($p \leq 0.05$) among means were determined by Duncan's

254   multiple range test (DMRT).

255

256   # Results

257   **Characteristics of biosorbents**

258   We found that RH had a higher specific surface area and total pore volume (4.24 $m^2 g^{-1}$, 0.0051

259    $cm^3 g^{-1}$) than RF (2.85 $m^2 g^{-1}$, 0.0043 $cm^3 g^{-1}$), while the average pore diameter of RH (4.824 nm)

260   was smaller than that of RF (5.997 nm), as indicated in Table 1. The pore size distribution of RF

261   and RH is shown in Fig 1.

262

263   **Adsorption of rice flour-methyl salicylate (RF-MeSA) and rice husk-methyl salicylate (RH-**

264   **MeSA)**

265   **Adsorption percentage**

266   The adsorption percentages of both RF-MeSA and RH-MeSA increased rapidly during hours 1-6

267   and then attained equilibrium between hours 12 and 24. At 24 h, the adsorption percentages of

268   RF-MeSA and RH-MeSA were 36.76 % and 58.33 %, respectively (Fig 2). The adsorption

269   percentage of RH-MeSA was significantly higher than that of RF-MeSA throughout the entire 24

270   h period ($p \leq 0.05$).

271

272 **Surface morphology**

273 The surface morphologies of RF and RH before and after MeSA adsorption (RF-MeSA and RH-

274 MeSA) were investigated by SEM, as shown in Fig 3A-D. According to the SEM images, RF

275 had pores and cracked surfaces on some parts of the starch granules, whereas pores were

276 significantly reduced on RF-MeSA. In addition, RH showed a longitudinal shape with a very

277 rough texture, while the surface of RH-MeSA was characterized by smooth channels. The EDS

278 spectrum confirmed the MeSA adsorption on the RF and RH surfaces. The RH content showed

279 carbon (71.11 %), oxygen (26.67 %), and potassium (2.22 %) atoms. After MeSA adsorption, the

280 RF-MeSA showed an increase in carbon content (84.91 %) (Fig 3E-F). The RH-MeSA showed a

281 higher carbon (29.58 %) and oxygen content (11.83 %) after the adsorption process than RH

282 (carbon=38.46 and oxygen=39.60 %) (Fig 3G-H).

283

284 **X-ray diffraction**

285 The XRD patterns (Fig 4A and B) present the structure of RF and RH before and after MeSA

286 adsorption. The main peaks for RF occurred at 2θ diffraction angles of 15°, 17°, 19°, and 23°;

287 these peaks indicate an A-type pattern of semi-crystalline structural arrangement of the amylose

288 and amylopectin molecules. After adsorption, the diffraction peak intensity of RF-MeSA

289 increased at 17°, 19°, and 23°, while RH-MeSA showed an increase in the peak intensity at 22°

290 and a slight shift in peak position from 18° to 14°. The crystalline structure patterns of both RF-

291 MeSA and RH-MeSA persisted.

292

293 **Functional groups**

294 We used FTIR to monitor vibrational frequency changes in the functional groups of RF-MeSA

295 and RH-MeSA, as shown in Fig 5A and B. The results showed different patterns in both RF and

296 RH before and after MeSA adsorption. Prior to adsorption, the peak at 3460 cm^{-1} for RF was

297 assigned to the vibration of O-H stretching, and the peak at 2900 cm^{-1} was assigned to C-H

298 stretching. The carbonyl group (C=O) of the esterified acetyl group was verified by the peak at

299 1740 cm^{-1}, and the peak at 1080 cm^{-1} was attributed to C-OH stretching of cellulose. For RH, the

300 adsorption peak at 3460 cm^{-1} was assigned to free hydroxyl groups present in cellulose,

301 hemicellulose, and lignin. The C-H stretching vibration at 2900 cm^{-1} indicated the presence

302 of an alkane functional group. The peak around 1740 cm^{-1} was assigned to C=O stretching,

303 which can be attributed to aromatic groups in the hemicelluloses and lignin. The FTIR

304 spectra of RF-MeSA and RH-MeSA did not show peaks at 3460 cm^{-1} (O-H stretching), but

305 rather at 3200 cm^{-1}, which corresponds with the spectrum of MeSA. The peak at 2900 cm^{-1} was

306 reflective of C-H stretching on both RF-MeSA and RH-MeSA.

307

308 **Thermogravimetric analysis**

309 The differences in weight loss of RF-MeSA and RH-MeSA were investigated by TGA curves,

310 which were separated into three phases (Fig 6A and B). The weight loss shown by RF within the

311 temperature range of 40-100 °C was attributed to the loss of water; that which occurred in the

312 temperature range of 180-350 °C corresponded to the degradation of the saccharide rings; and

313 thermal decomposition above 400 °C corresponded to char yields. In addition, the TGA curve of

314 RF-MeSA showed two peaks in phase 2. The first peak showed thermal decomposition of the

315 MeSA compound at around 155 °C, which resulted in a weight loss of 40.94 %. The second peak

316 was attributed to degradation of the saccharide rings. For RH, the peak in phase 1 was caused by

317   water evaporation. The peak in phase 2 indicated the degradation of hemicellulose and cellulose

318   between the temperatures of 180 °C and 400 °C. The degradation of lignin occurred over a

319   temperature range of 350 °C to 800 °C. The TGA curve of RH-MeSA showed a weight loss of

320   57.38 %, which corresponded to thermal decomposition of the MeSA compound at 155 °C.

321   Similarly, the TGA curve of MeSA confirmed that the weight loss that occurred at 155 °C (96.54

322   %) could be attributed to the thermal decomposition of the MeSA compound.

323

324   **Desorption of rice flour-methyl salicylate (RF-MeSA) and rice husk-methyl salicylate (RH-**

325   **MeSA)**

326   **Effect of temperature and relative humidity on desorption**

327   The effect of temperature on percentage of desorption was monitored for 24 h **(**Fig 7A). The

328   desorption percentages of RF-MeSA and RH-MeSA both significantly increased with

329   temperature increases from 25 °C to 40 °C, at 75 % relative humidity ($p \leq 0.05$).

330   The desorption percentage of RF-MeSA and RH-MeSA, induced by relative humidity, is shown

331   in Fig 7B. The percentage of desorption significantly increased with increasing relative humidity

332   ($p \leq 0.05$). At 75 % relative humidity, the desorption percentage of RF-MeSA was higher than

333   that of RH-MeSA. At 95 % relative humidity; the maximum desorption percentages for RF-

334   MeSA and RH-MeSA were 52.94 % and 49.03 %, respectively.

335

336   **Release kinetics**

337   The correlation coefficient (R^2) and release exponent (n) of the zero-order, first-order, Higuchi,

338   and Korsmeyer-Peppas models of RF-MeSA and RH-MeSA are summarized in Table 2. For

339   polymeric matrices, n ≤ 0.5 corresponds to a Fickian diffusion mechanism, and $0.5 < n < 1$ to a

340   non-Fickian mechanism. Table 2 shows that n-values less than 0.5 indicate that RF-MeSA and

341   RH-MeSA released at different temperatures (25 °C and 40 °C, respectively) and relative

342   humidities (75 % and 90 %, respectively); this finding is in line with Fickian diffusion

343   mechanisms. Moreover, a comparison of the R^2 values showed that the model best fitting the

344   release of RF-MeSA and RH-MeSA was the Higuchi model (R^2: 0.7734-0.9065). These results

345   suggest that the controlled release of MeSA can be described as a diffusion mechanism.

346

347   **Postharvest quality of banana fruit**

348   Both RF-MeSA and RH-MeSA were applied as biosorbents to delay the ripening of bananas (Fig

349   8). Bananas are a climacteric fruit and display a sharp increase in both ethylene production and

350   respiration rate after harvest; these are two factors that accelerate ripening (Seymour et al.,

351   1993). Our results showed that RH-MeSA and RF-MeSA treatments inhibited ethylene

352   production for 1 d of storage, with the control treatment exhibiting a significantly higher value

353   (34.72 ng kg^{-1} s^{-1}; $p \leq 0.05$). On d 3 of storage, the climacteric peak of ethylene production in the

354   control treatment was 1,465.28 ng kg^{-1} s^{-1}, while those of RH-MeSA and RF-MeSA were

355   1,198.62 and 1,144.44 ng kg^{-1} s^{-1}, respectively (Fig 9A). The respiration rate, which was 1.28 µg

356   kg^{-1} s^{-1} at harvest, increased in stored fruit. The respiration rate did not change significantly

357   throughout the storage period (Fig 7B). However, the yellowness (*b** value) of the control

358   treatment was significantly higher than that of the other treatments on d 3 and d 5 of storage ($p \leq$

359   0.05; Fig 9C). Similarly, the banana fruit firmness at harvest was 35.16 N and significantly

360   decreased during storage, reaching final values of 2.62 N in control fruit and significantly higher

361   values of 2.84 and 5.32 N in RF-MeSA and RH-MeSA treatments, respectively ($p \leq 0.05$; Fig

362 7D). Moreover, the half-life release (the time taken to release 50 % MeSA from the RF and RH)

363 was 4 d and 5 d at 25 °C and 75 % relative humidity, respectively. (Table 3)

364

Discussion

366 These results indicate that RH has higher specific surface area and total pore volume than RF. This

367 is likely due to the fact that the main organic compounds comprising RH are silica, cellulose,

368 hemicellulose, and lignin. This composition results in increased surface area and pore volume

369 (Ghosh & Bhattacherjee, 2013). According to the IUPAC classification of pore size as

370 macroporous (>50 nm), mesoporous (2.0-50 nm), and microporous (<2.0 nm), the average pore

371 diameter of RF and RH was 5.997 nm and 4.824, respectively. Therefore, RF and RH were

372 classified as mesoporous materials. The result can be explained because all sites on the biosorbents

373 were available at the initial stage of the process (Villacañas et al, 2006), which allowed MeSA

374 molecules to readily occupy them until the adsorption process stabilized, as reflected by the

375 attainment of equilibrium between 12 and 24 h. However, the time required to achieve equilibrium

376 in the adsorption process largely depends on the adsorbent structure and is influenced by the molar

377 mass of the adsorbed compound (Singh & Yenkie, 2006). Removing the excess MeSA compound

378 using Whatman® filter paper No.1 has particle retention at 98 % efficiency (Hutten, 2015) and it

379 did not affect the loss of active compounds that were trapped in the pores. This method has been

380 used to estimate the removal of heavy metal ions (Khokhotva & Waara 2010) and olive oil waste

381 (Garcia et al. 2006). Our results showed a higher specific surface area and total pore volume for

382 RH than for RF, which may account for the higher adsorption percentage recorded for RH-MeSA

383 relative to RF-MeSA. The XRD of RH showed strong broad peaks of semi-crystalline structures

384 at 2θ angle values of 18° and 22°. These peaks indicate the presence of cellulose fiber and silica

385   in the semi-crystalline structure (Kusbiantoro et al., 2012). Hence, the SEM images and EDS

386   spectrum confirmed that MeSA was adsorbed on the outer surface of RF and RH. The EDS

387   indicated from the increased amount of carbon after MeSA adsorption on both RF and RH that

388   MeSA was loaded on RF and RH successfully. In addition, the FTIR spectra indicated the

389   conjugated aromatic C-C, C=O, and hydrogen bonds that were the functional groups of the MeSA

390   compound, thereby confirming that RF and RH adsorbed the MeSA compound. The TGA implied

391   that MeSA could be adsorbed on RF and RH, and the amount of weight loss of RF-MeSA and RH-

392   MeSA was larger than the RF and RH samples. This result more clearly indicates that weight loss

393   is related to thermal degradation of adsorbed MeSA molecules. RH-MeSA showed a higher weight

394   loss than RF-MeSA, which can be attributed to the greater specific surface area and total pore

395   volume. During the adsorption process, the MeSA molecule attaches to the active sites of the

396   adsorbent surface and then it diffuses into the pores. Therefore, adsorption increases with the

397   surface area and pore volume of the adsorbent (Zhang & Blum, 2003). In addition, the percentage

398   of MeSA released from RH and RF increased with increasing temperature because of the weak

399   adsorptive forces between the binding sites of the adsorbent and adsorbate (Ofomaja & Ho, 2007).

400   Chen et al. (2010) reported that the hydrogen bonds between starch chains are broken and the

401   crystalline region is damaged with an increase in temperature. The humidity also affects the release

402   rate of RF-MeSA and RH-MeSA because RF and RH are hygroscopic materials (Navaratne, 2013).

403   Under high humidity, RF and RH have the ability to absorb and retain water molecules from the

404   air, leading to the displacement of MeSA molecules by water vapor (Smith et al., 1987). Therefore,

405   increasing the relative humidity leads to an increase in the release of the MeSA compound. The

406   temperature and relative humidity are important factors for controlling the release system. In

407   Thailand, the ambient temperatures are 25-40 °C and relative humidity is 75-85 %, while the

408   optimum relative humidity for the majority of fruit and vegetables are 90-95 % (McGregor, 1989).

409   Fruit and vegetables remain as living organs after harvested, and they continue to respire, leading

410   to moisture loss via the transpiration process (Ben-Yehoshua, 1969). Even though, these

411   biosorbent materials effectively delay the ripening of fruit, their application as biosorbents should

412   be balanced against the accelerated release of MeSA from the moisture from fresh produce.

413   The efficiencies of RF and RH were assessed as new biosorbents for controlling the release of

414   methyl salicylate (MeSA). In a closed system, 1 g dosages of adsorbents were investigated,

415   showing a pattern of Fickian diffusion. Therefore, RF-MeSA and RH-MeSA at 1 g adsorbents

416   dosage were applied to two bananas that were placed inside a PP tray. The half-life release (the

417   time for 50 % MeSA to be released from the RF and RH) was 4 and 5 d at 25 °C and 75 % relative

418   humidity. The application of RF-MeSA and RH-MeSA for delaying the ripening of 'Namwa'

419   banana fruit indicated that RH-MeSA and RF-MeSA inhibited the ethylene production of

420   'Namwa' bananas during storage. MeSA inhibits ethylene biosynthesis by blocking the conversion

421   of 1-aminocyclopropane-1-carboxylic acid (ACC) to ethylene (Leslie & Romani, 1986). Ethylene

422   plays a major role in regulating the ripening and softening of climacteric fruit such as mangos,

423   peaches, and jujubes (Srivastava & Dwivedi, 2000; Li et al., 2007). Thus, the inhibition of ethylene

424   production may suppress the ripening process and, thereby, maintain fruit firmness and delay color

425   change. However, the RF-MeSA and RH-MeSA treatment had no significant effect on respiration

426   rate. Ding and Wang (2003) reported that tomatoes treated with MeSA vapor (0.5 mmol L^{-1})

427   depressed their respiration rate from 18 to 6 $\mu g\ kg^{-1}\ s^{-1}$ compared to control fruit at 20 °C. Similarly,

428   MeSA vapor at 1.0 mmol L^{-1} reduced the respiration rate (6.94 $\mu g\ kg^{-1}\ s^{-1}$) of 'Primulat' sweet

429   cherries over 14 d, at 2 °C (Castillo et al., 2015). In our results, the banana fruit under both

430   treatments showed a slight change in the peel (red orange color). The application of RH-MeSA led

431 to a delayed ripening process compared with that of RF-MeSA; this was because the structure of

432 RH showed greater surface area and pore volume than RF, which affected the amount of MeSA

433 adsorbed on the surface (Sing et al., 1985). Moreover, a comparison of desorption percentages

434 showed a higher overall release in RF than in RH (at 25 °C, 75 % relative humidity), indicating

435 greater retention and therefore slower release of the MeSA compound on the part of the RH

436 biosorbent. Both RF and RH have already been used as biosorbents without modifying the surface.

437 RF-MeSA and RH-MeSA at 1 g of adsorbent dosage promoted adsorption of the MeSA at 36.76

438 % and 58.33 %, respectively and their ability to slowly release MeSA depended upon higher

439 temperatures and higher relative humidity. The half-life clearly confirmed the release of MeSA

440 from the RF and RH biosorbents and the diffusion was observed to be Fickian. Because RF and

441 RH are eco-friendly and innovative they are expected to replace the traditional adsorbents such as

442 β-CD which are obtained from the enzymatic degradation of starch (Lee et al., 2020). MeSA

443 inclusion with complex β-CD at 1:1 showed the highest MeSA entrapment efficiency (59 %),

444 indicating that the MeSA release increased with increasing relative humidity and temperature

445 (Kant et al. 2004). However, RF and RH have the potential to be similar to β-CD but without the

446 need for modification.

447

448 **Conclusions**

449 MeSA (1.0 g) was applied to RF and RH at a ratio of 2:1 (w/w; MeSA: biosorbent) at 25 °C for

450 24 h in order to reach equilibrium in the desorption process during postharvest treatment. Both

451 RF and RH have the potential to adsorb the MeSA molecule, as well as to release it. RH has a

452 higher specific surface area and total pore volume than RF, resulting in an increased capacity to

453 adsorb MeSA. Analysis with SEM, XRD, FTIR, and TGA confirmed the adsorption of MeSA on

454   the outer surfaces of RF and RH. Moreover, the temperature and relative humidity affected the

455   desorption percentage of RF-MeSA and RH-MeSA. Increased temperature (from 25 °C to 40 °C

456   at a relative humidity of 75 %) and increased relative humidity (from 75 % to 95 % at 25 °C)

457   stimulated the release of MeSA from RH-MeSA and RF-MeSA. In addition, the kinetically

458   controlled release of both RF-MeSA and RH-MeSA suggested that they followed a pattern of

459   Fickian diffusion. Thus, we report for the first time that RF and RH are natural adsorbents that

460   have potential applicability for the adsorption and controlled release of MeSA without chemical

461   or mechanical modifications. Although the application of RF-MeSA and RH-MeSA delayed

462   ripening of 'Namwa' banana fruit, treatments at the tested concentrations induced peel disorder.

463   Therefore, further study on pH, optimal dosage and concentration of MeSA are needed before

464   these biosorbents are utilized for commercial treatment with bananas or other fruit.

465

Acknowledgments

467   This research work was supported by The Thailand Research Fund (PHD60I0003). The authors

468   would like to thanks Nugreen Co., Ltd. (Thailand) for partially financial support and also like to

469   express their gratitude to Prof. Paul Holford (Western Sydney University) for his assistance in

470   proofreading this article.

471

References

473   Ahmad MZ, Akhter S, Ahmad I, Singh A, Anwar M, Shamim M, Ahmad FJ. 2012. *In vitro* and *in*

474   *vivo* evaluation of Assam Bora rice starch-based bioadhesive microsphere as a drug carrier for colon

475   targeting. Expert Opinion on Drug Delivery 9: 141-149. DOI: 10.1517/17425247.2012.633507.

476   Almenar E, Auras R, Rubino M, Harte B. 2007. A new technique to prevent the main post harvest

477   diseases in berries during storage: Inclusion complexes β-cyclodextrin-hexanal. The International

478   Journal of Food Microbiology 118: 164-172. DOI: 10.1016/j.ijfoodmicro.2007.07.002.

479   AOAC 2000. Moisture in cereal adjuncts: air oven method 945.15, 17th, ed. AOAC Official

480   Methods of Analysis.

481   Ariyanto HD, Bercis MN, Yoshii H. 2019. Effect of 1-methylcyclopropene release from

482   inclusion complexes powder on the quality of tomato by short-term treatment. IOP Conference

483   Series: Earth and Environmental Science 309: 012065. DOI: 10.1088/1755-1315/309/1/012065.

484   Bagnato N, Barrett R, Sedgley M, Klieber A. 2003. The effects on the quality of Cavendish

485   bananas, which have been treated with ethylene of exposure to 1-methylcyclopropene.

486   International Journal of Food Science & Technology 38: 745-750. DOI: 10.1046/j.1365-

487   2621.2003.00726.x.

488   Bansiwal AK, Rayalu SS, Labhasetwar NK, Juwarkar AA, Devotta S. 2006. Surfactant modified

489   zeolite (SMZ) as a slow release fertilizer for phosphorus. Journal of Agricultural and Food

490   Chemistry 54: 4777-4779. DOI: 10.1021/jf060034b.

491   Bartlet-Hunt SL, Knappe DRU, Barlaz MA. 2008. A review of chemical warfare agent simulants

492   for the study of environmental behaviour. Critical Reviews in Environmental Science and

493   Technology 38: 112-136. DOI: 10.1080/10643380701643650.

494   Basha EA, Hashim R, Mahmud HB, Muntohar AS. 2005. Stabilization of residual soil with

495   rice husk ash and cement. Construction and Building Materials 19: 448-453. DOI:

496   10.1016/j.conbuildmat.2004.08.001.

497   BeMiller JN, Pratt GW. 1981. Sorption of water, sodium sulfate, and water-soluble alcohols by

498   starch granules in aqueous suspension. Cereal Chemistry 58: 517-520.

499   Ben-Yehoshua S. 1969. Gas exchange, transpiration, and the commercial deterioration in storage

500   of orange fruit. Journal of the American Society for Horticultural Science 94: 524-528.

501   Bochek AM. 2003. Effect of hydrogen bonding on cellulose solubility in aqueous and

502   nonaqueous solvents. Russian Journal of Applied Chemistry 76: 1711-1719. DOI:

503   10.1023/B:RJAC.0000018669.88546.56.

504   Bouzayen M, Latché A, Nath P, Pech JC. 2010. Mechanism of fruit ripening. In Plant

505   Developmental Biology-Biotechnological Perspectives, pp. 319-339, Berlin, Heidelberg:

506   Springer.

507   Brunaue S, Emmett PH, Teller E. 1983. Adsorption of gases in multimolecular layers. Journal of

508   the American Chemical Society 60: 309-319. DOI: 10.1021/ja01269a023.

509   Castillo S, Valverde JM, Guillén F, Zapata PJ, Díaz-Mula HM, Valero D, Martínez-Romero D,

510   Serrano M. 2015. Methyl jasmonate and methyl salicylate affect differentially the postharvest

511   ripening process of 'Primulat' sweet cherry. Acta Horticulturae 1079: 541-544. DOI:

512   10.17660/actahortic.2015.1079.72.

513   Cevallos PAP, Buera MP, Elizalde BE. 2010. Encapsulation of cinnamon and thyme essential

514   oils components (cinnamaldehyde and thymol) in β-cyclodextrin: Effect of interactions with

515   water on complex stability. journal of food engineering 99: 70-75. DOI:

516   10.1016/j.jfoodeng.2010.01.039.

517   Chanjirakul K, Wang SY, Wang CY, Siriphanich J. 2006. Effect of natural volatile compounds

518   on antioxidant capacity and antioxidant enzymes in raspberries. Postharvest Biology and

519   Technology 40: 106-115. DOI: 10.1016/j.postharvbio.2006.01.004.

520   Chen P, Yu L, Simon GP, Liu X, Dean K, Chen L. 2011. Internal structures and phase-

521   transitions of starch granules during gelatinization. carbohydrate polymers 83: 1975-1983. DOI:

522   10.1016/j.carbpol.2010.11.001.

523   Chotikakham S, Faiyue B, Uthaibutra J, Saengnil K. 2019. Effects of methyl salicylate on

524   senescent spotting and hydrogen peroxide concentration in ripening 'Sucrier' bananas. Acta

525   Horticulturae 1245: 115-122. DOI: 10.17660/actahortic.2019.1245.17.

526   Ding CK, Wang CY, Gross KC, Smith DL. 2001. Reduction of chilling injury and transcript

527   accumulation of heat shock proteins in tomato fruit by methyl jasmonate and methyl salicylate.

528   Plant Science 161: 1153-1159. DOI: 10.1016/S0168-9452(01)00521-0.

529   Ding CK, Wang CY, Gross KC, Smith DL. 2002. Jasmonate and salicylate induce the expression

530   of pathogenesis-related-protein genes and increase resistance to chilling injury in tomato fruit.

531   Planta 214: 895-901. DOI: 10.1007/s00425-001-0698-9.

532   Ding CK, Wang CY. 2003. The dual effects of methyl salicylate on ripening and expression of

533   ethylene biosynthetic genes in tomato fruit. Plant Science 164: 589-596. DOI: 10.1016/S0168-

534   9452(03)00010-4.

535   Fatouros DG, Douroumis D, Nikolakis V, Ntais S, Moschovi AM, Trivedi V, Khima B, Roldo

536   M, Nazara H, Cox PA. 2011. In vitro and in silico investigations of drug delivery via zeolite

537   BEA. Journal of Materials Chemistry 21: 7789-7794. DOI: 10.1039/c1jm10204d.

538   Fernández-Pérez M, Villafranca-Sánchez M, Flores-Céspedes F, GarridoHerrera FJ, Pérez-

539   García S. 2005. Use of bentonite and activated carbon in controlled release formulations of

540   carbofuran. Journal of Agricultural and Food Chemistry 53: 6697-6703. DOI:

541   10.1021/jf051342x.

542   Fung RW, Wang CY, Smith DL, Gross KC, Tao Y, Tian M. 2006. Characterization of

543   alternative oxidase (AOX) gene expression in response to methyl salicylate and methyl

544   jasmonate pre-treatmentand low temperature in tomatoes. Journal of Plant Physiology 163: 1049-

545   1060. DOI: 10.1016/j.jplph.2005.11.003.

546   Fung RW, Wang CY, Smith DL, Gross KC, Tian M. 2004. MeSA and MeJA increase steady-

547   state transcript levels of alternative oxidase and resistance against chilling injury in sweet

548   peppers (*Capsicum annuum* L.). Plant Science 166: 711-719. DOI:

549   10.1016/j.plantsci.2003.11.009.

550   Garcia GM, Bachmann RT, Williams CJ, Burgoyne A, Edyvean RGJ. 2006. Olive oil waste as a

551   biosorbent for heavy metals. International Biodeterioration & Biodegradation 58: 231-238. DOI:

552   10.1016/j.ibiod.2006.06.028.

553   Geera BP, Nelson JE, Souza E, Huber KC. 2006. Composition and properties of A- and B-type

554   starch granules of wild-type, partial waxy, and waxy soft wheat. Cereal Chemistry 83: 551-557.

555   DOI: 10.1094/CC-83-0551.

556   Ghosh R, Bhattacherjee S. 2013. A review study on precipitated silica and activated carbon from

557   rice husk. Journal of Chemical Engineering & Process Technology 4: 156. DOI: 10.4172/2157-

558   7048.1000156.

559 Giménez MJ, Valverde JM, Valero D, Zapata PJ, Castillo S, Serrano M. 2016. Postharvest

560 methyl salicylate treatments delay ripening and maintain quality attributes and antioxidant

561 compounds of 'Early Lory' sweet cherry. Postharvest Biology and Technology 117: 102-109.

562 DOI: 10.1016/j.postharvbio.2016.02.006.

563 González Aguilar GA, Buta JG, Wang CY. 2003. Methyl jasmonate and modified atmosphere

564 packaging (MAP) reduce decay and maintain postharvest quality of papaya 'Sunrise'.

565 Postharvest Biology and Technology 28: 361-370. DOI: 10.1016/S0925-5214(02)00200-4.

566 Gray JE, Picton S, Giovannoni JJ, Grierson D. 1994. The use of transgenic and natural occurring

567 mutants to understand and manipulate tomato fruit ripening. Plant, Cell and Environment 19:

568 557-571. DOI: 10.1111/j.1365-3040.1994.tb00149.x.

569 Greenspan L. 1977. Humidity fixed-points of binary saturated aqueous-solutions. Journal of

570 Research of the National Bureau of Standards, Section A 81: 89-96. DOI:

571 10.6028/jres.081A.011.

572 Hamadi NK, Swaminathan S, Chen XD. 2004. Adsorption of Paraquat dichloride from aqueous

573 solution by activated carbon derived from used tires. Journal of Hazardous Materials 112: 133-

574 141. DOI: 10.1016/S0168-3659(02)00171-2.

575 Han J, Tian SP, Meng XH, Ding ZS. 2006. Response of physiologic metabolism and cell

576 structures in mango fruit to exogenous methyl salicylate under low-temperature stress.

577 Physiologia Plantarum 128: 125-133. DOI: 10.1111/j.1399-3054.2006.00731.x.

578   Ho BT, Joyce DC. Bhandari BR. 2011. Release kinetics of ethylene gas from ethylene-α-

579   cyclodextrin inclusion complexes. Food Chemistry 129: 259-266. DOI:

580   10.1016/j.foodchem.2011.04.035.

581   Hoffman AS. 2008. The origins and evolution of controlled drug delivery systems. Journal of

582   Controlled Release 132: 153-163. DOI: 10.1016/j.jconrel.2008.08.012.

583   Hutten IM. 2015. Handbook of Nonwoven Filter Media.Oxford: Butterworth-Heinemann.

584   Journal of the Science of Food and Agriculture 81: 1244-1249. DOI: 10.1002/jsfa.933.

585   Kamada M, Hirayama F, Udo K, Yano H, Arima H, Uekama K. 2002. Cyclodextrin conjugate-

586   based controlled release system: Repeated-and prolonged-releases of ketoprofen after oral

587   administration in rats. Journal of Controlled Release 82: 407-416. DOI: 10.1016/S0168-

588   3659(02)00171-2.

589   Kant A, Linforth RS, Hort J, Taylor AJ. 2004. Effect of β-cyclodextrin on aroma release and

590   flavor perception. Journal of Agricultural and Food Chemistry 52: 2028-2035. DOI:

591   10.1021/jf0307088.

592   Kawagoe R, Takikawa Y, Hikosaka O. 1998. Expectation of reward modulates cognitive signals

593   in the basal ganglia. Nature Neuroscience 1: 411-416. DOI: 10.1038/1625.

594   Khan AS, Singh Z, Abbasi NA. 2007. Pre-storage putrescine application suppresses ethylene

595   biosynthesis and retards fruit softening during low temperature storage in "Angelino" plum.

596   Postharvest Biology and Technology 46: 36-46. DOI: 10.1016/j.postharvbio.2007.03.018.

597   Khokhotva O, Waara S. 2010. The influence of dissolved organic carbon on sorption of heavy metals

598   on urea-treated pine bark. Journal of Hazardous Materials15: 689-96. DOI:

599   10.1016/j.jhazmat.2009.08.149.

600   Korsmeyer RW, Gurny R, Doelker E, Buri P, Peppas NA. 1983. Mechanism of solute release

601   from porous hydrophilic polymers. International Journal of Pharmaceutics 15: 25-35. DOI:

602   10.1016/0378-5173(83) 90064-9.

603   Kusbiantoro A, Nuruddin MF, Shafiq N, Qazi SA. 2012. The effect of microwave incinerated

604   rice husk ash on the compressive and bond strength of fly ash based geopolymer concrete.

605   Construction and Building Materials 36: 695-703. DOI: 10.1016/j.conbuildmat.2012.06.064.

606   Lee M, Dey KP, Lee YS. 2020. Complexation of methyl salicylate with β-cyclodextrin and its

607   release characteristics for active food packaging. Food Science and Biotechnology 29: 917-925.

608   DOI: 10.1007/s10068-020-00749-z.

609   Lee YS, Chung DS, Harte BR, Shin J. 2010. Effect of 1-methylcyclopropene (1-MCP) treatment

610   on the quality characteristics and pigmentation of tomato fruit (*Lycopersicon esculentum mill*).

611   Korean Journal of Horticultural Science & Technology 28: 600-608.

612   Leslie CA, Romani RJ. 1986. Salicylic acid: a new inhibitor of ethylene biosynthesis. Plant Cell

613   Reports 5: 144-146. DOI: 10.1007/BF00269255.

614   Li Z, Zhang Y. 2010. Use of surfactant-modified zeolite to carry and slowly release sulfate.

615   Desalination and Water Treatment 21: 73-78. DOI: 10.5004/dwt.2010.1226.

616 Li Z. 2003. Use of surfactant-modified zeolite as fertilizer carriers to control nitrate release.

617 Microporous and Mesoporous Materials 61: 181-188. DOI: 10.1016/S1387-1811(03)00366-4.

618 López-Rubio A, Almenar E, Hernandez-Munoz P, Lagaron JM, Catala R, Gavara R. 2004.

619 Overview of active polymer-based packaging technologies for food applications. Food Reviews

620 International 20: 357-387. DOI: 10.1081/FRI-200033462.

621 Mason L, Moore RA, Edwards JE, McQuay HJ, Derry S, Wiffen PJ. 2004. Systematic review of

622 efficacy of topical rubefacients containing salicylates for the treatment of acute and chronic pain.

623 British Medical Journal 328: 995. DOI: 10.1136/bmj.38040.607141.EE.

624 McGregor BM. 1989. Tropical products transport handbook. USDA Office of Transportation.

625 Agricultural Handbook 668.

626 Min D, Li F, Zhang X, Shu P, Cui X, Dong L, Ren C, Meng D, Li J. 2018. Effect of methyl salicylate

627 in combination with 1-methylcyclopropene on postharvest quality and decay caused by *Botrytis*

628 *cinerea* in tomato fruit. Journal of the Science of Food and Agriculture 98: 3815-3822. DOI:

629 10.1002/jsfa.8895.

630 Mir N, Canoles M, Beaudry R, Baldwin E, Pal Mehla C. 2004. Inhibiting tomato ripening with

631 1-methylcyclopropene. Journal of the American Society for Horticultural Science 129: 112-120.

632 DOI: 10.21273/JASHS.129.1.0112.

633 Mulugeta M, Lelisa B. 2014. Removal of methylene blue (Mb) dye from aqueous solution by

634 bioadsorption onto untreated parthenium hystrophorous weed. Modern Chemistry & Applications 2-4

635 DOI: 10.4172/2329-6798.1000146.

636   Namazi H, Bahrami S, Entezami AA. 2005. Synthesis and controlled release of biocompatible

637   prodrugs of β-cyclodextrin linked with PEG containing ibuprofen or indomethacin. Iranian Polymer

638   Journal 14: 921-927.

639   Navaratne S. 2013. Selection of polymer based packing material in packing of hygroscopic food

640   products for long period of storage. European International Journal of Science and Technology 2:

641   1-7.

642   Ofomaja AE, Ho YS, 2007. Equilibrium sorption of anionic dye from aqueous solution by palm

643   kernel fibre as sorbent. Dyes and Pigments 74: 60-66. DOI: 10.1016/j.dyepig.2006.01.014.

644   Pratt HK, Goeschl JD. 1969. Physiological roles of ethylene in plants. Annual Review of Plant

645   Physiology 20: 541-548.

646   Prawingwong P, Chaiya C, Reubroycharoen P, Samart C. 2009. Utilization of rice husk ash silica

647   in controlled releasing application. Journal of Metals, Materials and Minerals 19: 61-65.

648   Ryals JA, Neuenschwander UH, Willits MG, Molina A, Steiner HY, Hunt MD. 1996. Systemic

649   acquired resistance. Plant Cell 8: 1809-1819.

650   Santander-Ortega MJ, Stauner T, Loretz B, Ortega-Vinuesa JL, Bastos-González D, Wenz C,

651   Schaefer UF, Lehr CM. 2010. Nanoparticles made from novel starch derivatives for transdermal

652   drug delivery. Journal of Controlled Release 141: 85-92. DOI: 10.1016/j.jconrel.2009.08.012.

653   Satirapipathkul C, Meesukanun K. 2013. Controlled Release of *Atractylodes lancea* extract from

654   rice starch-konjac glucomannan film. Advanced Materials Research 747: 186-189. DOI:

655   10.4028/www.scientific.net/AMR.747.186.

656   Sayyari M, Babalar M, Kalantari S, Martínez-Romero D, Guillén F, Serrano M, Valero D. 2011.

657   Vapour treatments with methyl salicylate or methyl jasmonate alleviated chilling injury and

658   enhanced antioxidant potential during postharvest storage of pomegranates. Food Chemistry 124:

659   964-970. DOI: 10.1016/j.foodchem.2010.07.036.

660   Seymour GB, Taylor JE, Tucker GA. 1993. Biochemistry of fruit ripening. London: Chapman and

661   Hall Publishers.

662   Sing KSW, Everet DH, Haul RAW, Moscou L, Pierotti RA, Rouquerol J. 1985. Reporting

663   physisorption data for gas/solid systems with special reference to the determination of surface area

664   and porosity. Pure and Applied Chemistry 57: 603-619. DOI: 10.1002/9783527610044.hetcat0065.

665   Singh S, Yenkie MKN. 2006. Scavenging of priority organic pollutants from aqueous waste

666   using granular activated carbon. Journal of the Chinese Chemical Society 53: 325-334. DOI:

667   10.1002/jccs.200600041.

668   Smith JP, Ooraikul B, Koersen WJ, van de Voort FR, Jackson ED, Lawrence RA. 1987. Shelf

669   life extension of a bakery product using ethanol vapor. Food Microbiology 4: 329-337. DOI:

670   10.1016/S0740-0020(87)80007-2.

671   Srivastava MK, Dwivedi UN. 2000. Ripening of banana fruit by salicylic acid. Plant Science

672   158: 87-96. DOI: 10.1016/S0168-9452(00)00304-6.

673   Takeo KI, Kuge T. 1969. Complexes of starchy materials with organic compounds: Part III. X-

674   ray studies on amylose and cyclodextrin complexes. Agricultural and Biological Chemistry 33:

675   1174-1180. DOI: 10.1080/00021369.1969.10859434.

676 Tareen MJ, Abbasi NA, Hafiz IA. 2012. Postharvest application of salicylic acid enhanced

677 antioxidant enzyme activity and maintained quality of peach cv. Flordaking fruit during storage.

678 Scientia Horticulturae 142: 221-228. DOI: 10.1016/j.scienta.2012.04.027.

679 Teranishi K, Shimomura O. 2014. Solubilizing coelenterazine in water with hydroxypropyl-β-

680 cyclodextrin. Bioscience, Biotechnology, and Biochemistry 61: 1219-1220. DOI:

681 10.1271/bbb.61.1219.

682 Tramer M.R. 2004. It's not just about rubbing-topical capsaicin and topical salicylates may be

683 useful as adjuvants to conventional pain treatment. British Medical Journal 328: 998. DOI:

684 10.1136/bmj.328.7446.998.

685 Trichard L, Delgado-Charro MB, Guy RH, Fattal E, Bochot A. 2007. Novel beads made of alpha-

686 cyclodextrin and oil for topical delivery of a lipophilic drug. Pharmaceutical Research 25: 435-440.

687 DOI: 10.1007/s11095-007-9395-0.

688 Ugheoke BI, Mamat O. 2012. A novel method for high volume production of nano silica from

689 rice husk: Process development and product characteristics. International Journal of Materials

690 Engineering Innovation 3: 139-155. DOI: 10.1504/IJMATEI.2012.046898.

691 Vilar G, Tulla-Puche J, Albeicio F. 2012. Polymers and drug delivery systems. Current Drug

692 Delivery 9: 1-28. DOI: 10.2174/156720112801323053.

693 Villacañas F, Pereira MFR, Órfao JJM, Figueiredo JL. 2006. Adsorption of simple aromatic

694 compounds on activated carbons. Journal of Colloid and Interface Science 293: 128-36. DOI:

695 10.1016/j.jcis.2005.06.032.

696   Xiaoyu N, Yuejin W, Zhengyan W, Lin W, Guannan Q, Lixiang Y. 2013. A novel slow-release urea

697   fertiliser: Physical and chemical analysis of its structure and study of its release mechanism.

698   Biosystems Engineering 115: 274-282. DOI: 10.1016/j.biosystemseng.2013.04.001.

699   Yang SF, Hoffman NE. 1984. Ethylene biosynthesis and its regulation in higher plants. Annual

700   Reviews of Plant Physiology 35: 155-189. DOI: 10.1146/annurev.pp.35.060184.001103.

701   Yebra DM, Kiil S, Dam-Johansen K. 2004. Antifouling technology-past, present and future steps

702   towards efficient and environmentally friendly antifouling coatings. Progress in Organic

703   Coatings 50: 75-104. DOI: 10.1016/j.porgcoat.2003.06.001.

704   Zhang B, Blum FD. 2003. Thermogravimetric study of ultrathin PMMA films on silica: effect of

705   tacticity. Thermochimica Acta 396: 211-217.

Figure 1

Pore size distribution of rice flour (RF) and rice husk (RH).

 Chemistry Journals
Analytical, Inorganic, Organic, Physical, Materials Science
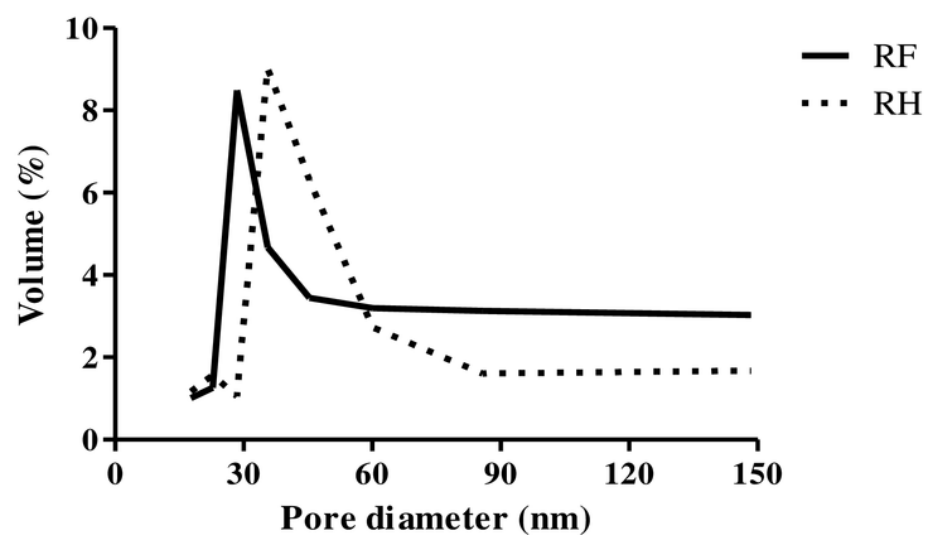
Figure 2

The percentage adsorption of rice flour-methyl salicylate (RF-MeSA) and rice husk-methyl salicylate (RH-MeSA) at 25 °C for 24 h.
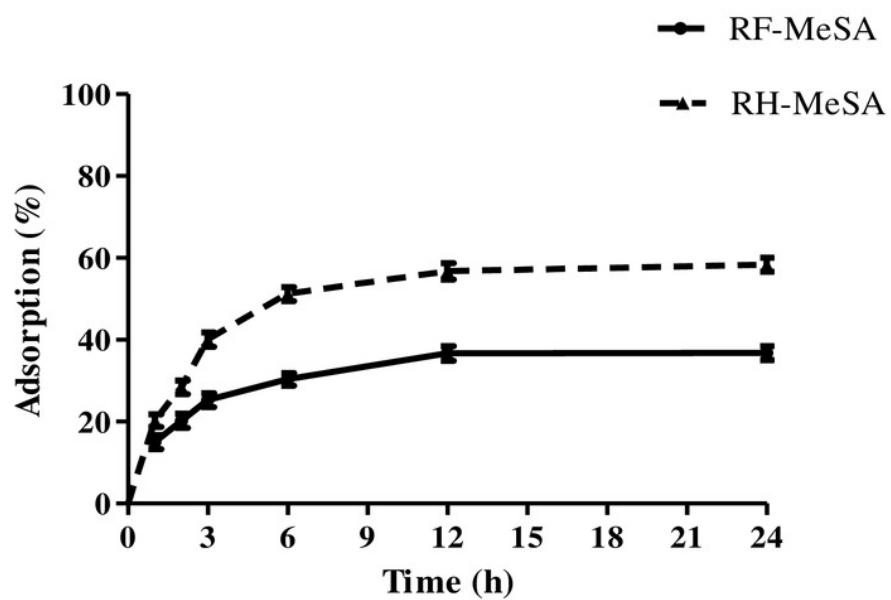
Figure 3

SEM images and EDS spectrum of rice flour (RF) (A), rice flour-methyl salicylate (RF-MeSA) (B), rice husk (RH) (C), and rice husk-methyl salicylate (RH-MeSA) (D) at 24 h.
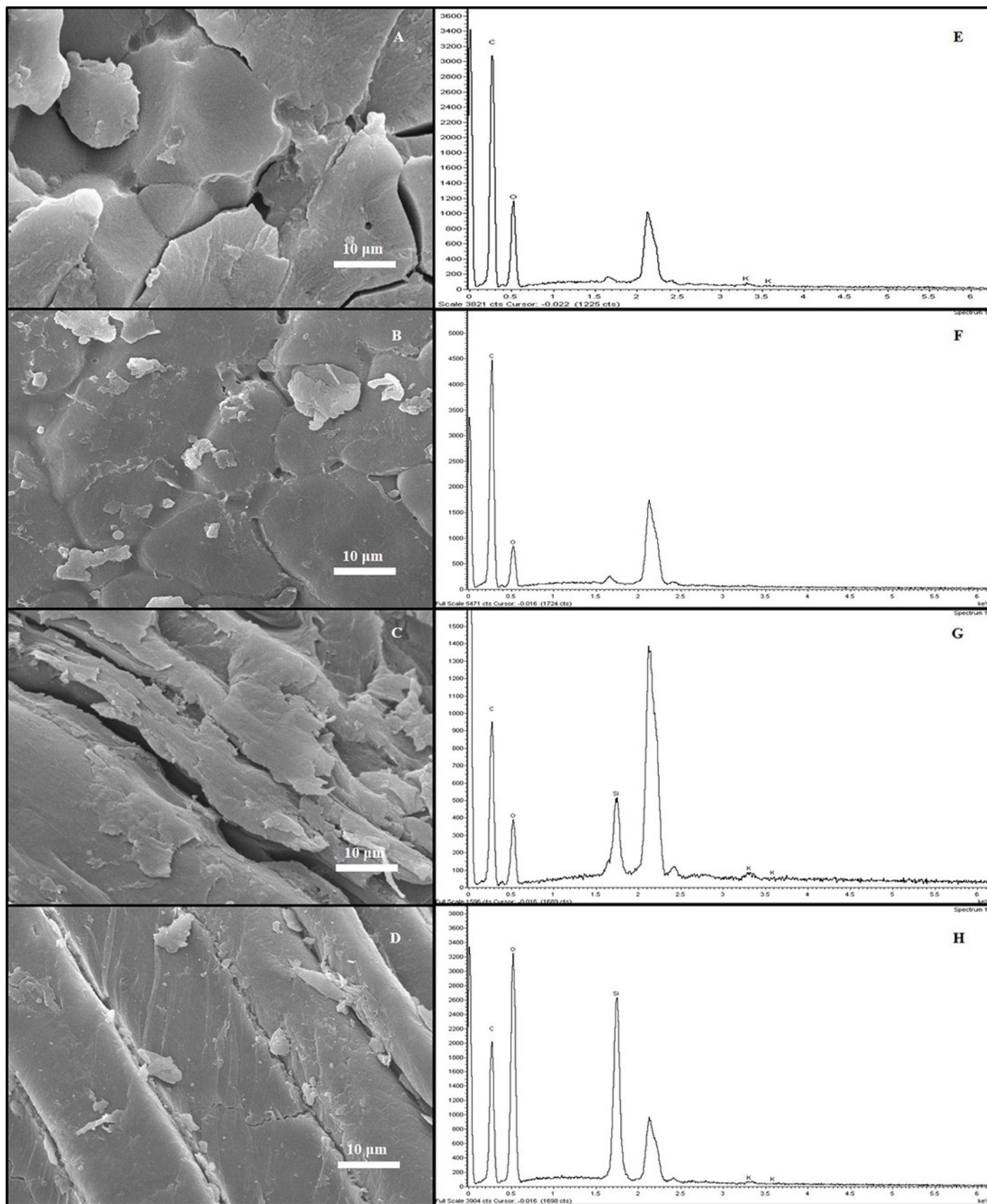
Figure 4

XRD patterns of rice flour (RF) and rice flour-methyl salicylate (RF-MeSA) at 24 h. (A), rice husk (RH) and rice husk-methyl salicylate RH-MeSA (B) at 24 h.
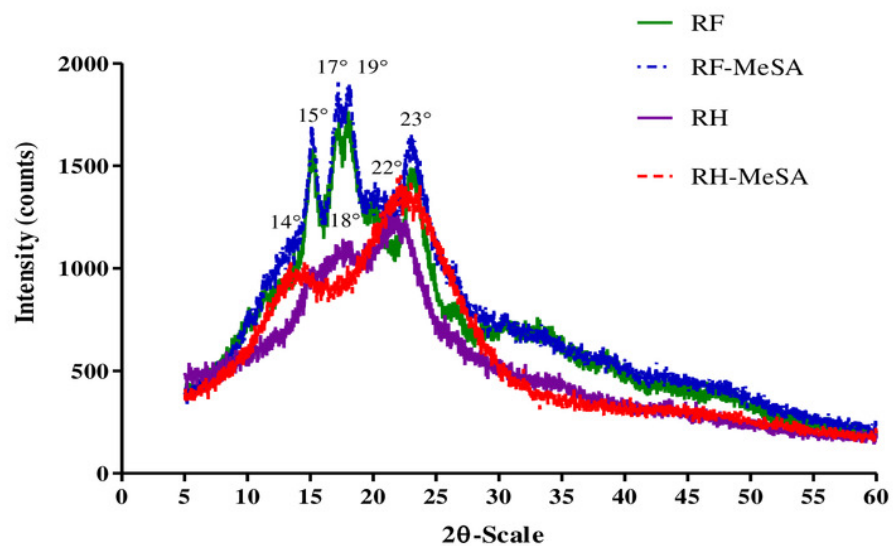
Figure 5

FTIR spectra of rice flour-methyl salicylate (RF-MeSA) at 24 h. (A), rice husk (RH) and rice husk-methyl salicylate RH-MeSA (B) at 24 h.
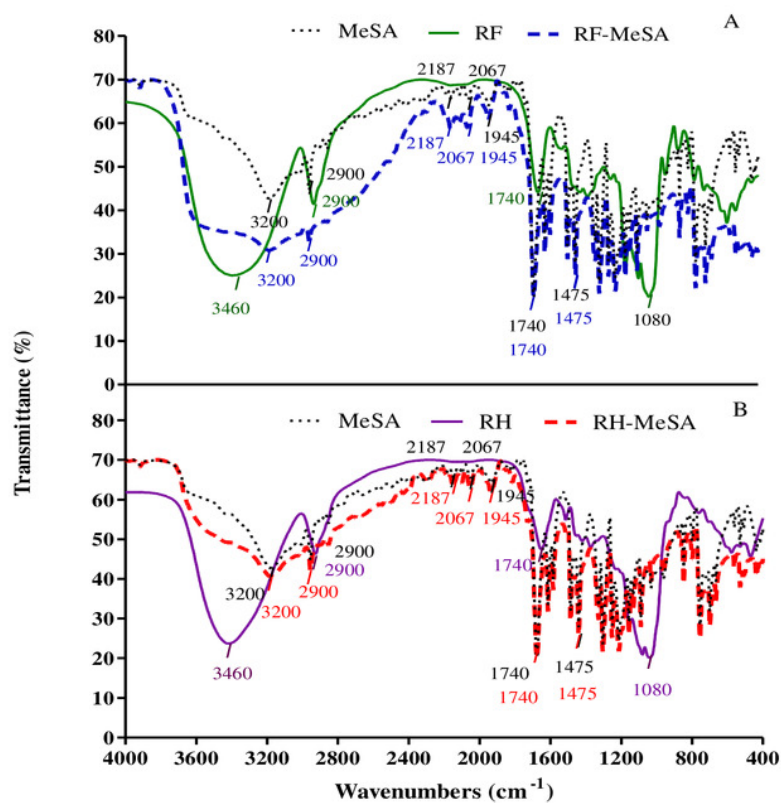
Figure 6

TGA curve of rice flour (RF) and rice flour-methyl salicylate (RF-MeSA) at 24 h. (A), rice husk (RH) and rice husk-methyl salicylate RH-MeSA (B) at 24 h.

PeerJ **Chemistry Journals**
Analytical, Inorganic, Organic, Physical, Materials Science
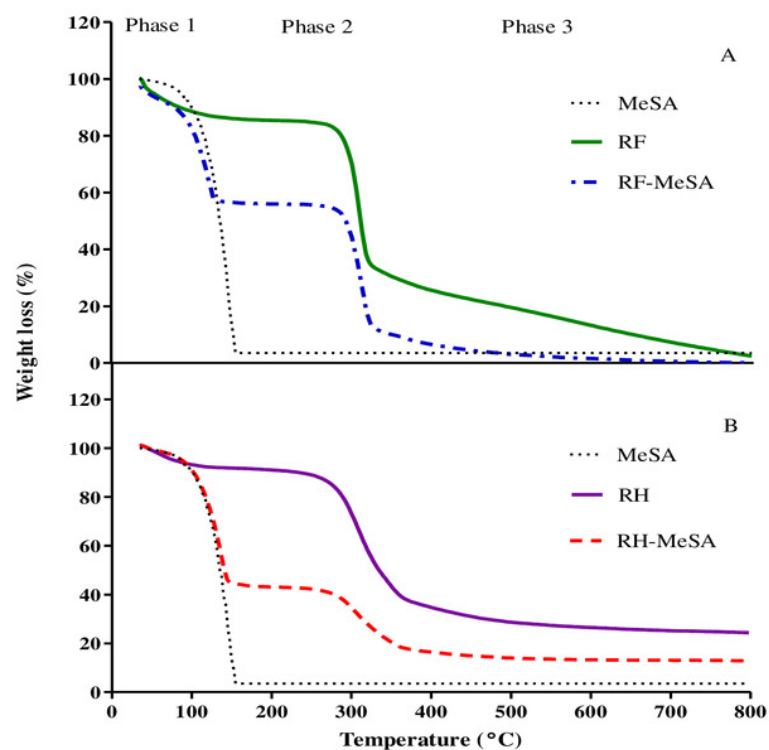
Figure 7

The percentage desorption of rice flour-methyl salicylate (RF-MeSA) and rice husk-methyl salicylate (RH-MeSA).

(A) The percentage desorption of rice flour-methyl salicylate (RF-MeSA) and rice husk-methyl salicylate (RHMeSA) at different temperatures (25 °C and 40 °C), relative humidity at 75 %.

(B) The percentage desorption of rice flour-methyl salicylate (RF-MeSA) and rice husk-methyl salicylate (RHMeSA) at different relative humidity (75 % and 95 %), at 25 °C.
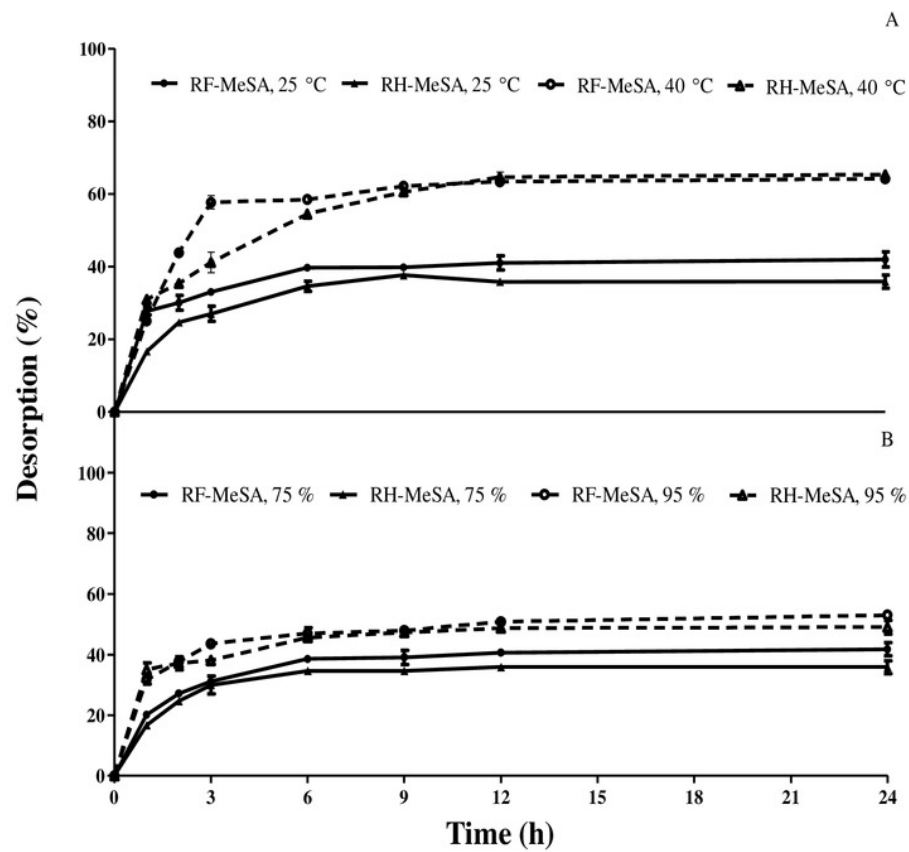
Figure 8

Visual peel color changes of banana fruit before, during, and after the postharvest treatment with RF-MeSA, RH-MeSA and untreated fruit (control) during storage at 25 ± 2 °C.
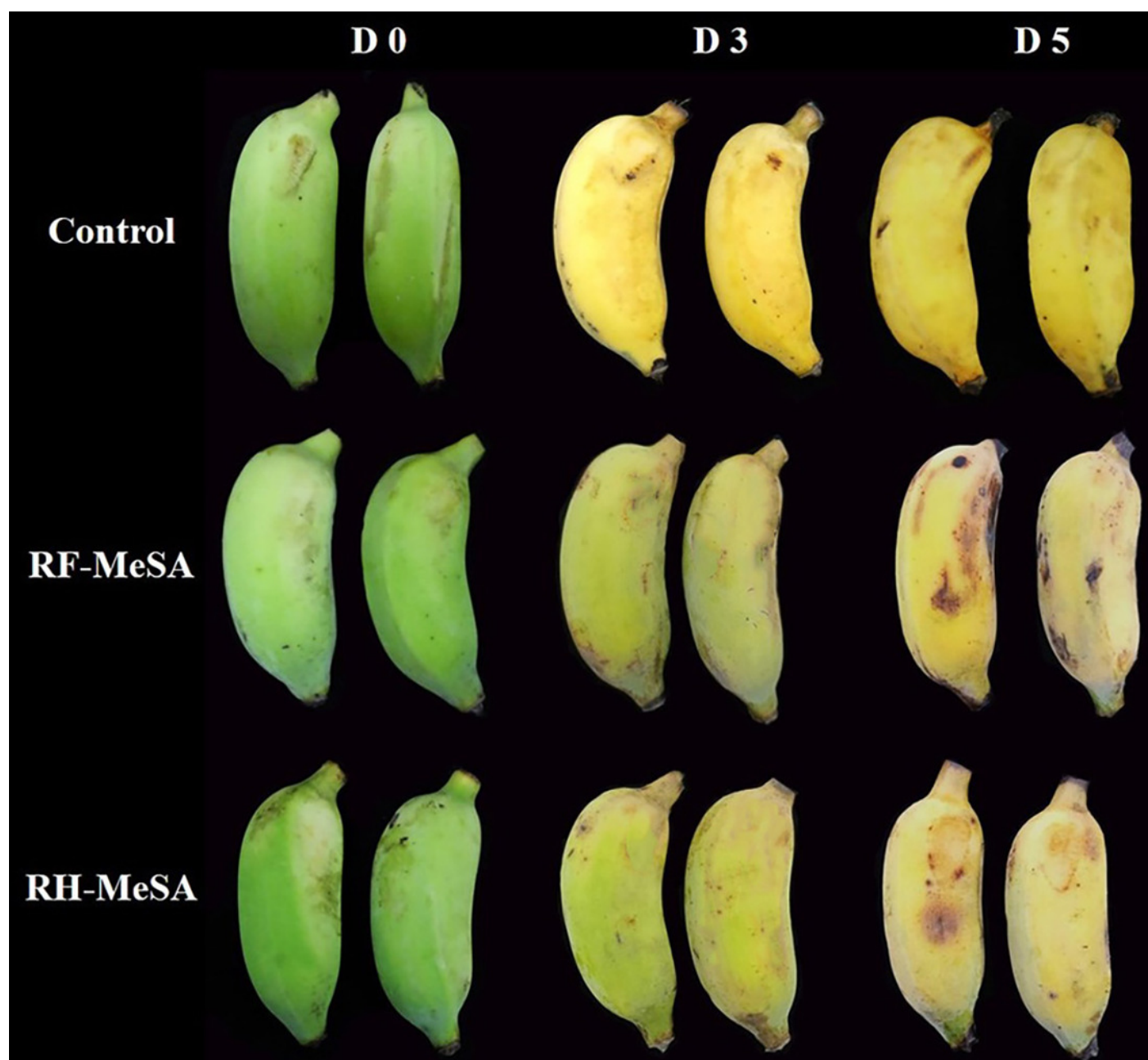
BET surface area of rice flour (RF) and rice husk (RH).

Parameters	Biosorbents	
	RF	RH
Specific surface area ($m^2 \ g^{-1}$)	2.850±0.002	4.240±0.003
Total pore volume ($cm^3 \ g^{-1}$)	0.0043±0.0021	0.0051±0.0027
Average pore diameter (nm)	5.997±1.428	4.824±1.485

 Chemistry Journals
Analytical, Inorganic, Organic, Physical, Materials Science

Correlation coefficient (R^2) according to different models and release exponent (n).

Correlation coefficient (R^2) according to different models and release exponent (n) used to describe the release of rice flour-methyl salicylate (RF-MeSA) and rice husk-methyl salicylate (RH-MeSA) at different temperatures (25 °C and 40 °C) and relative humidity (75 % and 95 %).

Models	RF-MeSA				RH-MeSA			
	Temperature (°C)		Relative humidity (%)		Temperature (°C)		Relative humidity (%)	
	25	40	75	95	25	40	75	95
Zero-order (R^2)	0.4876	0.5539	0.5334	0.5652	0.5269	0.6992	0.5352	0.4854
First-order (R^2)	0.4907	0.5829	0.5382	0.5934	0.5348	0.7203	0.5434	0.5024
Higuchi (R^2)	0.7734	0.8128	0.8340	0.8352	0.8169	0.9065	0.8164	0.7717
Korsmeyer-Peppas (R^2)	0.7799	0.8161	0.7800	0.7194	0.7503	0.8745	0.7180	0.6951
n	0.25	0.58	0.35	0.35	0.27	0.57	0.23	0.30

Half-life values of the methyl salicylate (MeSA) compound to release from the rice flour (RF) and rice husk (RH) biosorbent.

Half-life	Biosorbents	
	RF	RH
$t_{1/2}$ (d)	4	5